



Proceedings of ICACTCE'21

High School of Technology, Moulay Ismail University Meknes, Morocco, and
Faculty of Sciences and Techniques Mohammeda, Hassan II University, Morocco
March 24 – 26, 2021, Morocco

Editors: Mariyam Ouaisa, Mariya Ouaisa, Sarah El Himer, and Zakaria Boulouard

Research Article

Effect of UV-Light Illumination on Room Temperature ZnO Nanotubes for Ethanol Gas Sensing

B. Ydir^{*1}, O. Boualiouaat¹, H. Lahlou¹, M. Bousseta¹, Es-Said Akhouayri¹,
V. Fierro², A. Celzard² and D. Prades³

¹ LETSMP, Department of Physics, Faculty of Science, Université Ibn Zohr, Agadir 80000, Morocco

² N2EV, Department of Nanomaterials, Electronics and Vivant-Institut Jean Lamour, UMR 7198 CNRS-UL, Epinal, France

³ Department of Electronic and Biomedical Engineering, University of Barcelona, Barcelona, Spain

Abstract. A gas sensor based on force spun ZnO nanotube was successfully developed by using a simple and cost-effective approach, as confirmed by SEM, EDS, TGA-DTG and XRD characterization techniques. In order to optimize the sensing performance of the device in terms of sensing response kinetics and stability, the sensor response behavior against ethanol vapor was investigated under dark and UV light. Different reported studies have demonstrated that the resistance of ZnO gas sensors towards ethanol decreases when it is exposed to UV light. In this work, the UV light illumination of the sensor at 370 nm, allowed effectively to activate the detection of ethanol at the ppm level at room-temperature, in contrast to dark conditions. Unexpectedly, it was observed that the resistance behavior of the prepared ZnO sensor was reversed under continuous UV irradiation. The sensing mechanism behind this change is being also discussed.

Keywords. Forcespinning; ZnO; Nanotubes; Ethanol; Gas sensor; UV-light activation; Room temperature

PACS. 81.16.-c; 07.07.Df; 91.67.Vf

Copyright © 2020 B. Ydir, O. Boualiouaat, H. Lahlou, M. Bousseta, Es-Said Akhouayri, V. Fierro, A. Celzard and D. Prades. *This is an open access article distributed under the Creative Commons Attribution License, which permits unrestricted use, distribution, and reproduction in any medium, provided the original work is properly cited.*

*Corresponding author: b.ydir.96@gmail.com

1. Introduction

Gas sensors based on *Metal Oxide* (MOx) materials have proven to be an excellent choice for a diverse range of applications related to the protection of human health and public safety, including food quality analysis, toxic gas monitoring, pollution control, and biomedical diagnostics, etc. [2,3,6]. In this sense, ethanol is one of the hazardous and flammable compounds widely used in chemical processes and whose concentration should be controlled at the ppm level to ensure human safety [5].

The controllable synthesis of one-dimensional MOx nanomaterials (such as nanotubes, nanofibres, nanowires, etc.) allowed them to be excellent candidates for gas sensing purposes [4, 8, 12]. More particularly, 1D MOx ultrafine tubes are expected to offer high sensitivity due to their high length-to-diameter ratio and surface-to-volume ratio. Among the metal oxides, ZnO is one of the best candidates for gas sensing applications, due to its controlled morphology, tunable sensing parameters, light transparency, cost-effectiveness and non-toxicity.

In a previous work, a cost-effective approach based on Forcespinning was recently applied for the first time to produce different 1D MOx sensing materials using a simple home-made apparatus [4]. The successful production of highly porous ZnO nanotubes was demonstrated using this technique [4]. Moreover, this latter offers a high production rate and, its flexibility makes it favorable for gas sensor mass production at the industrial scale [12].

The prepared sensor showed good sensitivity but slow response kinetics, towards ethanol, under thermo-activation in the range of 180 °C to 250 °C [4,10]. Moreover, as stated in literature, the prolonged exposure of the sensor to heating at such temperatures, may induce a thermal degradation of the sensitive layer, thereby affecting the stability and the lifetime of the sensing device [11]. Then, lowering the sensing temperature of metal oxide gas sensors, while keeping good response kinetics is quite attractive but is still a challenging task [13].

Many solutions have been implemented in literature to solve these problems, such as the doping of ZnO with transition elements and noble metals or its surface modification by other metal oxides or carbonaceous materials [1, 9, 13]. Recently, continuous and pulsed UV light illumination has been proposed as simpler and promising alternative to achieve near room-temperature operation of some ZnO-based gas sensors [11]. In addition, it has been shown that the detection features of UV-Visible LED sensors could be tailored depending on the illumination parameters of the sensor [7].

In this contribution, we focus on the development of ZnO ultrafine tubes based gas sensors toward the detection of ethanol. In an attempt to find a good compromise between improved signal to noise ratio, fast response kinetics and fair sensor stability toward ethanol at the ppm level, the sensing performance of the sensor is investigated under three different activation modes, namely: thermo-activation, light-activation and combined activation. The sensing behavior of the device under the three different modes are compared and discussed and the optimal sensor working parameters are being selected.

2. Experimental

2.1 Sensor Preparation

Polyvinylpyrrolidone (PVP) with a molecular weight of 1.300.000 was used as fiber molding polymer. Zinc acetate dehydrate ($\text{Zn}[\text{COOCH}_3]_2 \cdot 2\text{H}_2\text{O}$) was used as a precursor material for ZnO synthesis. Firstly, 0.7 g of $\text{Zn}[\text{COOCH}_3]_2 \cdot 2\text{H}_2\text{O}$ was dissolved in a 4 g mixture of ethanol/N, N-dimethylformamide (1 : 1, wt/wt) (S_1). Meanwhile, 2 g of PVP was dissolved in a 4 g mixture of ethanol/N, N-dimethylformamide (1 : 1, wt/wt) under mechanical stirring for 2 h (S_2). Subsequently, (S_1) was added to (S_2) drop-wise and stirred for 2h until the solution became clear.

During the forcespinning process, the final solution was feed into the centrifugal reservoir and ejected on the fiber collectors under the centrifugal force. In this process, the fibers were quickly transformed into microfibers due to the stretching induced by the centrifugal force and the solvent evaporation. During the fiber jet process, the distance between the two reservoir outlets (with an internal diameter of 200 μm) and the collectors was kept constant at 10 cm and, whereas the rotation rate of the tank was fixed at 10,000 rpm [12]. Afterwards, the as-spun fibers were annealed at 600 °C for 5h, with a heating rate of 5 C°·min⁻¹. Then, they were deposited by drop coating over a glass platform with interdigitated gold microelectrodes.

2.2 Material Characterization

Thermo-gravimetric and differential thermal analysis (TGA-DTA; Netzsch STA44F3A9) were used to investigate the thermal properties of the as-spun composite in air in the temperature range of 25 to 1000 °C. The *Scanning Electron Microscopy* (SEM) images combined with *Energy Dispersive X-ray Spectroscopy* (EDS) analysis were performed using a JEOL JSM-6700F Scanning Electron Microscope. The XRD patterns were obtained using a Bruker D8 Advanced X-ray Diffractometer with Cu-K α radiation ($\lambda = 1.54060 \text{ \AA}$).

2.3 Gas Sensor Characterization

In order to study the gas detection properties of the ZnO prepared sensor, a gas characterization system was developed, consisting of three essential parts, namely (Figure 1):

- A gas sampling circuit for the generation of pure carrier air at a constant flow.
- A gas sensing chamber equipped with a gas inlet and outlet, hosting the ZnO gas sensor and a commercial secondary sensor to monitor the temperature and humidity inside the chamber.
- An electronic control and data acquisition system.

During the whole measurement cycle, the carrier air flows across the chamber at a constant flow of 50 sccm adjusted using the *Mass flow controller* (MFC) system. After sensor resistance stabilization under air, the target ethanol vapor is injected into the test chamber with a well-defined concentration using a micro-syringe. The carrier air flowing across the chamber allows the sensor to recover its baseline resistance (Figure 1a).

Simultaneously, the sensor response under ethanol vapor is monitored by measuring the resistance evolution versus time using a voltage divider circuit (Figure 1b). The sensor response (%) was defined as the ratio $\left| \frac{R_a - R_g}{R_a} \right| * 100$, where R_a and R_g are the sensor resistance under air and ethanol vapor, respectively.

The sensor activation was performed by continuously exposing the sensor to Ultraviolet Light delivered by a commercial *Light Emitting Diode* (LED) at 370 nm, with an optical power of 26 mW. The light intensity of the LED was controlled by *Pulse Width Modulation* (PWM) by regulating the duty cycle from 0 to 100%. The LED control and sensor data acquisition were performed by an Arduino Mega programmable card controlled through a LabVIEW interface (Figure 1b).

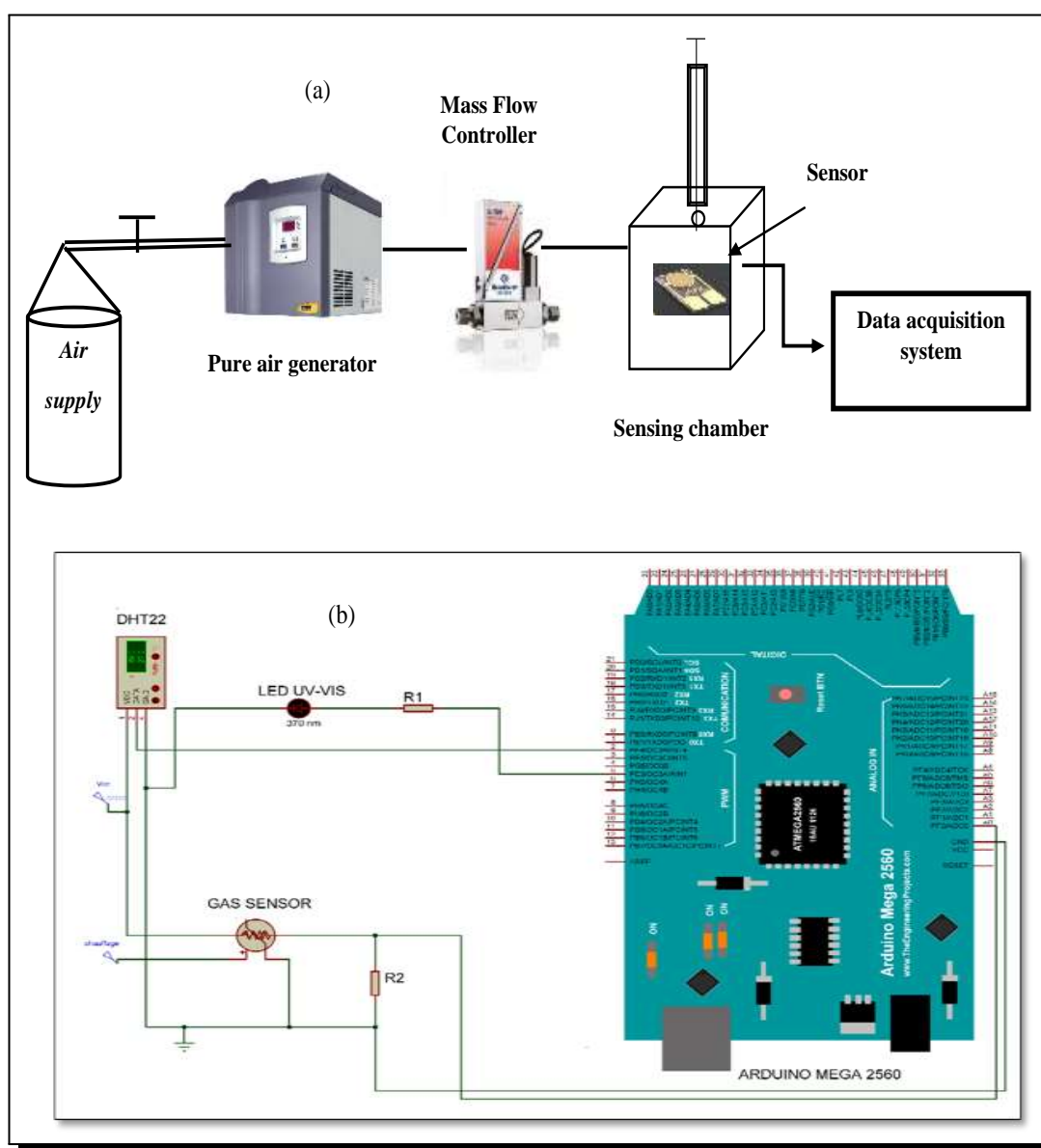


Figure 1. Experimental gas sensor characterization system, (a) Gas sampling circuit, (b) Electronic circuit

3. Results and Discussion

3.1 Material Morphology

Figure 2 shows the SEM images made on the as-spun Zn [COOCH₃]₂/PVP composite and the thermally annealed ZnO samples. As could be observed, the as-spun composite formed one-dimensional smooth microfibers (Figure 2a), which, after annealing, were converted into porous ZnO nanotubes with diameters in the range of 0.6-1 μm (Figure 2b), due to the removal of PVP polymer and the precursor oxidation.

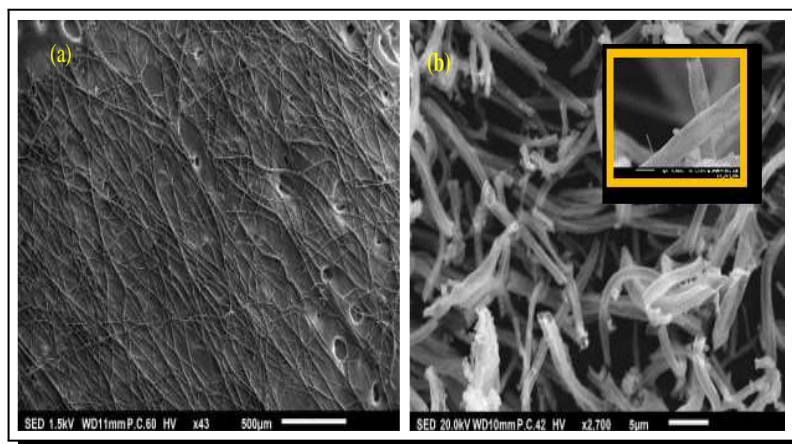


Figure 2. SEM images of (a) as-spun Zn [COOCH₃]₂/PVP composite, and (b) annealed ZnO sample

3.2 Thermo Gravimetric and EDS Analysis

The first minor weight loss before 180 °C could be attributed to the removal of the precursor free solvents (Figure 3a). Then, the significant weight loss of approximately 65%, observed between 180 °C and 500 °C, was attributed to the complete decomposition of Zn [COOCH₃]₂ and the degradation of PVP. The elemental EDS analysis, made on the annealed sample, confirmed the presence of Zn and O elements of ZnO, without any observed impurity or contamination (Figure 3b).

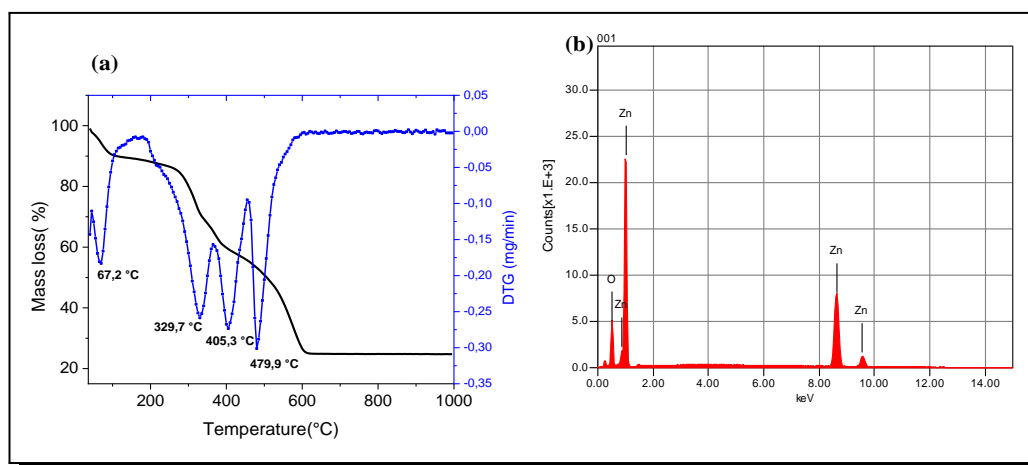


Figure 3. TGA-DTG curves of (a) the as-spun Zn [COOCH₃]₂·2H₂O/PVP sample, (b) The elemental EDS analysis of annealed ZnO sample

3.3 Material Crystallinity

XRD measurements were carried out to investigate the crystal structure of ZnO nanotubes annealed at 600 °C. The analysis obtained showed that ZnO crystallized following a unique zincite phase, and no peaks from any other phase were observed, which indicated that the prepared nanotubes are pure (Figure 4). Besides, ZnO presented a mean particle size of 30.87 nm, calculated according to the Debye-Scherer formula:

$$D = \frac{0.89\lambda}{\beta \cos\theta},$$

where λ is the wavelength of the used X-Ray source, β is the line broadening corresponding to the *Full Width Half Maximum* (FWHM) peak intensity and θ is the Bragg angle.

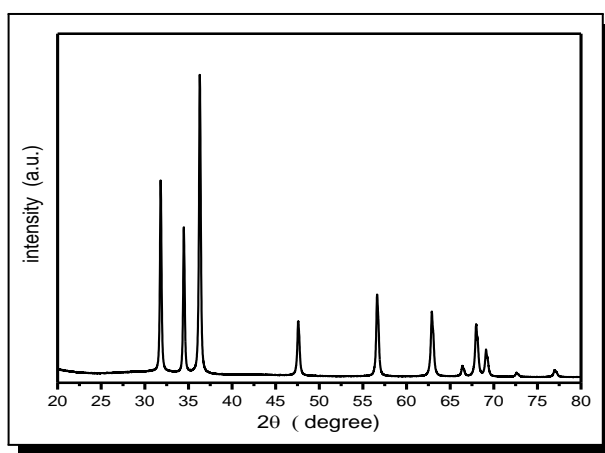


Figure 4. XRD patterns of annealed ZnO nanotubes

3.4 Gas Sensing Properties

The normalized resistance behavior of the ZnO nanotube sensor in the air under UV irradiation at 370 nm was studied. Figure 5 depicts the sensor response in the air as a function of time, in darkness (LED off) and under illumination using different duty cycle values (DC = 50, 75, 100%).

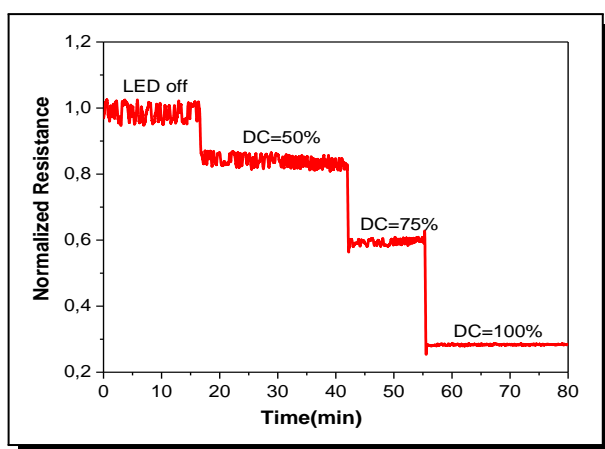


Figure 5. Evolution of sensor baseline resistance under air in darkness (LED off) and under illumination at different UV light intensities

Thus, compared to the sensor baseline in darkness, UV light resulted in a decrease in resistance as much as the UV light intensity was increased. This change in resistance is due to the increased generation of electron-hole pairs. This led to an increase in ZnO conductivity, hence a decrease in the baseline resistance, indicating the typical behavior of an *n*-type semiconductor under UV irradiation. Also, UV irradiation contributed in reducing the signal noise amplitude as much as the light intensity increased.

On the one hand, when exposed to ethanol at room-temperature under dark conditions, no response was observed in the range of 18 to 60 ppm. In fact, according to our previous work the sensor starts to be sensitive to ethanol vapor, under darkness, since the sensor temperature overcomes 180 °C [8]. As shown in Figure 6(a), the sensor showed a typical decrease in resistance under ethanol with a response magnitude around 80% and a response and recovery times of 111 seconds and 95 minutes, respectively.

On the other hand, the sensor resistance toward ethanol under UV irradiation is shown in Figure ??(b). In this case, activation is performed in continuous mode with a 100% duty cycle. In Contrast to the dark conditions, the sensor showed a change in resistance when exposed to ethanol at room-temperature, under UV irradiation.

After the ethanol injection, the sensor showed two subsequent reactions; first, a strong decrease in the resistance followed by a slower increase, before the initial baseline value was restored (Figure 6b). Indeed, as the ethanol concentration increased from 36 to 60 ppm, the first response magnitude (effect 1) appeared to be independent of the ethanol concentration. In turn, the second response (effect 2) appeared to increase proportionally. Clearly, the response to ethanol under UV irradiation was reversed. However, the sensor showed an improvement in the sensor response kinetics (response time of about 74 seconds, and recovery time of about 70 min) under UV at room-temperature, compared to the dark conditions at 180 °C. In turn, only a slight increase was observed in the response magnitude (from 80% in darkness to 85% under UV).

Compared to the first two modes of activation (thermo or UV light-activation), the use of the combined mode (UV light combined with heating at 180 °C) led to a considerable improvement of the sensor properties, in terms of response and recovery times (Figure 6c). In fact, the latter decreased from 111 seconds to about 4 seconds, while the former dropped from 95 minutes to 9 minutes. Thus, the UV illumination plays a crucial role in promoting the sensor reaction rate, because UV light can provide sufficient energy to desorb the chemisorbed oxygen species on ZnO surfaces. This was accompanied with a slight improvement of the response magnitude from 80 to 90%.

In summary, to get better results concerning the metrological properties of the sensor for ethanol detection, we recommend working with combined activation, using 180 °C with continuous UV irradiation (at 100% duty cycle).

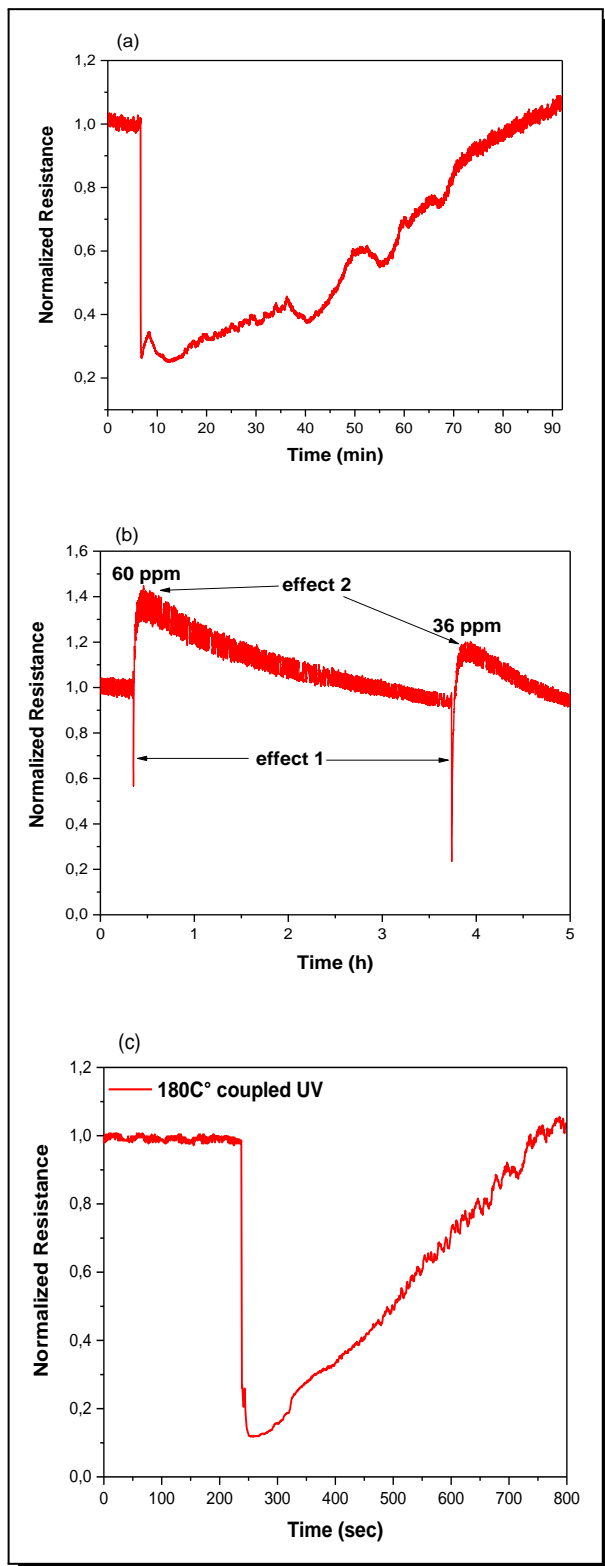
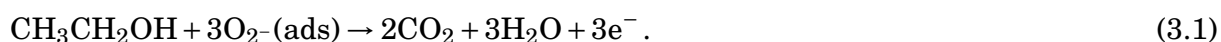


Figure 6. Normalized resistance behavior of ZnO, (a) under 60 ppm of ethanol at 180°C in dark conditions, (b) under 36 and 60 ppm of ethanol vapor at room-temperature under continuous UV illumination (DC = 100%), (c) under 60 ppm of ethanol at 180°C coupled with continuous UV (DC = 100%)

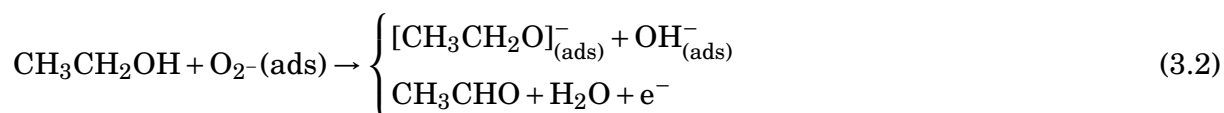
3.5 Sensing Mechanism

On one hand, at ambient temperature, the sensor didn't show any sensitivity to ethanol. Whereas the sensor showed a typical decrease in resistance when exposed to ethanol at a threshold temperature of 180 °C, as illustrated in Figure 6(a). This is due to the interaction of ethanol, known as a reducing vapor, with the surface oxygen species of the ZnO nanotubes (with *n*-type behavior), resulting in a decrease in the concentration of the oxygen surface species, and therefore an increase in the concentration of electrons, according to the typical reactions (3.1) and (3.2):



On another hand, when subjecting the sensor to UV light combined with heating at 180 °C, the observed response to ethanol can be attributed to the formation of photo-induced oxygen ions ($\text{O}_2^-(\text{ads})(h\nu)$). Indeed, during UV activation, the photo-induced ions react with ethanol according to reaction (3.1) and (3.2). As a result of this process, electrons are injected into the ZnO conduction layer, which reduces the sensor resistance.

By contrast to both previous cases, during UV irradiation at room-temperature, the dissociation of ethanol into aldehyde (CH_3CHO) and H_2O is more prominent than the formation of CO_2 and H_2O [13]. At room-temperature, the dehydrogenation of ethanol molecules generates OH^- ions (breaking of C–O bond) and $[\text{CH}_3\text{CH}_2\text{O}]^-$ ions (breaking of O–H bond) due to the lower bond breaking energy of C–O and O–H bonds. Ethanol vapor can be easily attached to metal oxide surfaces in the form of dehydrogenated ionic fragment $[\text{CH}_3\text{CH}_2\text{O}]^-$ through the interaction of adsorbed oxygen on metal oxide surfaces. These reactions result in a release of free electrons, thereby inducing a first decrease in the sensor resistance, as observed in Figure 6b, following reaction (3.2) [13]:



Then, the generated aldehyde covers the surface and decomposes catalytically. The aldehyde's subsequent decomposition leads to the secondary increase in the sensitive layer resistance, as illustrated in Figure 6b.

4. Conclusion

In summary, a sensitive gas sensor based on forcespun porous ZnO nanotubes is successfully developed. In order to improve the sensor lifetime and reduce its energy consumption, systematic measurement tests were carried out under ethanol vapor at room-temperature. The results show that the prepared ZnO sensor can detect ethanol in the ppm level at room-temperature under UV irradiation, with reduced signal noise and improved response kinetics, compared to our previous results obtained in dark conditions at much higher temperatures. Nevertheless, a behavior inversion of ethanol response was observed during UV irradiation at room-temperature,

compared to the classical response of ZnO toward ethanol. The sensing mechanism behind this effect was discussed according to the photoconduction properties of ZnO. This system could be further improved, in the future, by integrating other more powerful LEDs with different wavelengths. Other illumination frequencies could also be tested. This approach is expected to allow us obtaining more optimized detection properties and will open the way for the tuning of the sensor selectivity toward ethanol in the presence of other interfering gases.

Competing Interests

The authors declare that they have no competing interests.

Authors' Contributions

All the authors contributed significantly in writing this article. The authors read and approved the final manuscript.

References

- [1] V.M. Aroutiounian, Decrease in operation temperature of Zinc Oxide nanomarkers, *Biomedical Journal of Scientific & Technical Research* **30**(2) (2020), 23211 – 23220, DOI: 10.26717/BJSTR.2020.30.004919.
- [2] A. Beniwal and Sunny, Apple fruit quality monitoring at room-temperature using sol-gel spin coated Ni-SnO₂ thin film sensor, *Journal of Food Measurement and Characterization* **13**(1) (2019), 857 – 863, DOI: 10.1007/s11694-018-9998-7.
- [3] V.S. Bhati, M. Hojamberdiev and M. Kumar, Enhanced sensing performance of ZnO nanostructures-based gas sensors: a review, *Energy Reports* **6** (2020), 46 – 62, DOI: 10.1016/j.egyr.2019.08.070.
- [4] O. Bouaaliouat, H. Lahlou, E.-S. Akhouayri, A. Ihlal, A. Benlhachemi, D. Prades, V. Fierro, A. Celzard, F. Berger and J.-B. Sanche, Forcespun metal oxide ultrafine tubes for hazardous gas monitoring, *Materials Today: Proceedings* **27** (2020), 3124 – 3131, DOI: 10.1016/j.matpr.2020.04.009.
- [5] P.F. Cao, S.Y. Ma, X.L. Xu, B.J. Wang, Omer Almamoun, T. Han, X.H. Xu, S.T. Pei, R. Zhang, J.L. Zhang and W.W. Liu, Preparation and characterization of a novel ethanol gas sensor based on FeYO₃ microspheres by using orange peels as bio-templates, *Vacuum* **177** (2020), 109359, DOI: 10.1016/j.vacuum.2020.109359.
- [6] G. Korotcenkov and B.K. Cho, Metal oxide composites in conductometric gas sensors: achievements and challenges, *Sensors Actuators, B Chem.* **244** (2017), 182 – 210, DOI: 10.1016/j.snb.2016.12.117.
- [7] R. Kumar, X. Liu, J. Zhang and M. Kumar, Room temperature gas sensors under photoactivation: from metal oxides to 2D materials, *Nano-Micro Letters* **12**, Article number: 164 (2020), DOI: 10.1007/s40820-020-00503-4.
- [8] H. Lahlou, S. Claramunt, O. Monereo, D. Prades, J.-M. Fernandez-Sanjuá, N. Bonet, F.-M. Ramos and A. Cirer, Preparation of palladium oxide nanoparticles supported on tin oxide nanofibers via modified electrospinning for ultra-low ppb NO₂ detection, *Materials Today: Proceedings* **36** (2020), 1 – 9, DOI: 10.1016/j.matpr.2020.04.674.

- [9] S. Lulwani, A. Beniwal and Sunny, Enhancing room-temperature ethanol sensing using electrospun Ag-doped SnO₂-ZnO nanofibers, *Journal of Materials Science: Materials in Electronics* **3127** (2020), 17212 – 17224, DOI: 10.1007/s10854-020-04276-9.
- [10] Y.T. Ma, S. Ma, J. Tang, Z.G. Wu, J. Shi, Y. Zhao, S.T. Pei and P.F. Cao, Hydrothermal-synthesis flower-like SnS microspheres gas sensors bonded physically by PVDF for detecting ethanol, *Vacuum* **181** (2020), 109657, DOI: 10.1016/j.vacuum.2020.109657.
- [11] R. Ponnusamy, D. Sivasubramanian, P. Sreekanth, V. Gandhiraj, R. Philip and G.M. Bhalerao, Nonlinear optical interactions of Co: ZnO nanoparticles in continuous and pulsed mode of operations, *RSC Advances* **5**(98) (2015), 80756 – 80765, DOI: 10.1039/c5ra10756c.
- [12] K. Sarkar, C. Gomez, S. Zambrano, M. Ramirez, E. de Hoyos, H. Vasquez and K. Lozano, Electrospinning to ForcespinningTM, *Materials Today* **13**(11) (2010), 12 – 14, DOI: 10.1016/S1369-7021(10)70199-1.
- [13] P.P. Suha and M.K. Jayaraj, Enhanced room-temperature gas sensing properties of low temperature solution processed ZnO/CuO heterojunction, *BMC Chemistry* **13**, Article number: 4 (2019), 11 pages, DOI: 10.1186/s13065-019-0519-5.

